Amyloid β-Protein Oligomerization

PRENUCLEATION INTERACTIONS REVEALED BY PHOTO-INDUCED CROSS-LINKING OF UNMODIFIED PROTEINS*

Gal Bitan‡, Aleksey Lomakin§, and David B. Teplow‡¶

From the ‡Center for Neurologic Diseases, Brigham and Women's Hospital, and Department of Neurology (Neuroscience), Harvard Medical School, Boston, Massachusetts 02115 and the §Department of Physics, Center for Material Science and Engineering, and Materials Processing Center, Massachusetts Institute of Technology, Cambridge, Massachusetts 02139

Assembly of the amyloid β-protein (Aβ) into neurotoxic oligomers and fibrils is a seminal event in Alzheimer's disease. Understanding the earliest phases of Aβ assembly, including prenucleation and nucleation, is essential for the development of rational therapeutic strategies. We have applied a powerful new method, photoinduced cross-linking of unmodified proteins (PICUP), to the study of Aβ oligomerization. Significant advantages of this method include an extremely short reaction time, enabling the identification and quantification of short lived metastable assemblies, and the fact that no *pre facto* structural modification of the native peptide is required. Using PICUP, the distribution of Aβ oligomers existing prior to assembly was defined. A rapid equilibrium was observed involving monomer, dimer, trimer, and tetramer. A similar distribution was seen in studies of an unrelated amyloidogenic peptide, whereas nonamyloidogenic peptides yielded distributions indicative of a lack of monomer preassociation. These results suggest that simple nucleation-dependent polymerization models are insufficient to describe the dynamic equilibria associated with prenucleation phases of Aβ assembly.

Alzheimer's disease is a progressive, neurodegenerative disorder characterized in part by amyloid deposition in the cerebral neuropil and vasculature (1). Amyloid deposits contain abundant fragments and full-length (40 or 42 residues) forms of the amyloid β-protein (Aβ)[1] (for a review, see Ref. 2). Aβ is produced through endoproteolysis of the amyloid β-protein precursor (AβPP), a type I integral membrane protein (3). Compelling evidence indicates that factors that increase the production of Aβ (or of particularly amyloidogenic forms of the peptide) or that facilitate deposition or inhibit elimination of amyloid deposits cause Alzheimer's disease or are risk factors for the disease (4). Recently, evidence has emerged both from *in vitro* and *in vivo* studies that soluble, oligomeric forms of Aβ have potent neurotoxic activities and may, in fact, be the proximal effectors of the neuronal injury and death occurring in Alzheimer's disease (for a review, see Ref. 5). In addition, oligomers may be involved in other amyloid-associated, neurodegenerative diseases, including Huntington's (6) and Parkinson's (7). These new findings emphasize the importance of elucidating the mechanistic details of the Aβ oligomerization process in order to establish a knowledge base for the development of therapeutic strategies.

In vitro studies of Aβ assembly have revealed three main types of oligomers: 1) Aβ-(1–40) oligomers ranging from dimer through hexamer (8–10); 2) Aβ-derived diffusible ligands (ADDLs), oligomers of Aβ-(1–42) ranging in molecular mass between 17,000 and 42,000 Da (corresponding to tetramers through decamers) (11); and 3) protofibrils (PF), narrow, flexible, fibril intermediates formed by Aβ peptides and by at least nine other amyloidogenic peptides and proteins (12–21). The precursor-product relationships involving small oligomers, ADDLs, PF, and fibrils are not completely understood. Kinetic studies of the smallest oligomers (8–10) have not been conducted. Similarly, the relationship between ADDLs, small oligomers, and PF is not clear. Studies of Aβ PF have shown that these assemblies form from low molecular weight Aβ (thought to contain monomers or dimers), have secondary structures rich in β-sheet, and give rise to fibrils (13, 22, 23). Less is known about the biophysical properties of ADDLs (*e.g.* their equilibrium relationships with other assemblies and their conformational characteristics). In addition, it appears that ADDL formation is restricted to the 42-residue form of Aβ.

Studies of the size distribution of Aβ oligomers have not produced a consensus. Evidence for the existence of dimers and higher order oligomers was found initially in studies of synthetic Aβ peptides using size exclusion chromatography (SEC) (24, 25). Determination of the aggregation state was confounded by the tendency of the peptides to aggregate during the chromatography. In order to overcome this problem, Roher *et al.* (8) used concentrated formic acid and other denaturants in the SEC mobile phase. For example, Aβ dimers and trimers have been observed in material from amyloid plaques when 80% formic acid or 5 M guanidine thiocyanate was used (8, 26). Similar oligomers were produced *in vitro* upon incubation of synthetic Aβ-(1–42) at pH 7.4 (8). However, because highly acidic or chaotropic media can dissociate noncovalently associated oligomers and polymers, this approach does not allow determination of the native distribution of oligomers. In addi-

¶ To whom correspondence should be addressed: Center for Neurologic Diseases, Brigham and Women's Hospital, 77 Ave. Louis Pasteur (HIM 756), Boston, MA 02115-5716. Tel.: 617-525-5270; Fax: 617-525-5252; E-mail: teplow@cnd.bwh.harvard.edu.

[1] The abbreviations used are: Aβ, amyloid β-protein; AβPP, amyloid β-protein precursor; ADDL, Aβ-derived diffusible ligand; PF, protofibrils; SEC, size exclusion chromatography; LMW, low molecular weight; MWCO, molecular weight cut-off; PICUP, photoinduced cross-linking of unmodified proteins; HPLC, high performance liquid chromatography; PACAP, pituitary adenylate cyclase-activating polypeptide; GRF, growth hormone-releasing factor; CT, calcitonin; TTR, transthyretin; Ru(Bpy), Tris(2,2′-bipyridyl)dichlororuthenium(II); APS, ammonium persulfate; PAGE, polyacrylamide gel electrophoresis.

tion, although the resolution of SEC is sufficient to resolve monomers, dimers, and possibly trimers, from each other, it cannot resolve higher order oligomers, limiting its ability to provide an accurate determination of the oligomer size distribution.

Gel electrophoresis has revealed the presence of small oligomers *in vivo* (27), in conditioned media of certain cell lines (28–31), and using synthetic peptide preparations (13, 32). However, the approach is associated with significant interpretive caveats. First, the key principle upon which SDS gel electrophoresis depends is the dissociation of protein complexes and the denaturation of the resulting monomers. Dissociation of oligomeric and fibrillar Aβ by SDS is well known (13). Second, SDS may also have the counterintuitive effect of facilitating protein aggregation. Protocols for isolation of both Aβ and prion proteins take advantage of this property (33, 34), and Aβ oligomerization induced by SDS during SDS-PAGE has been shown previously (9). It is thus unlikely that oligomer distributions defined using SDS-PAGE accurately reflect the distributions existing prior to electrophoresis.

An equilibrium between Aβ monomers, tetramers, and possibly dimers has been proposed based on analytical ultracentrifugation measurements (32). This method is highly sensitive but is dependent on the global fitting of the data to multistate association models in order to produce information about oligomer distributions. In fact, these models predicted very similar results for theoretical monomer-dimer, monomer-trimer, or monomer-tetramer equilibria (32), making firm conclusions about the true oligomerization state of the peptide difficult. Recently, preparative fractionation of Aβ-(1–40) using noncontinuous gradient ultracentrifugation was found to produce a low molecular weight fraction containing peptide oligomers, but the distribution of oligomers could not be determined (35).

A number of spectroscopic approaches have been applied to the Aβ oligomerization problem. Measurement of the hydrodynamic radius of low molecular weight Aβ using dynamic light scattering suggested that Aβ exists as either a compact dimer or an extended monomer (36). However, despite the power of this method for monitoring aggregation noninvasively and in real time, the molecular weight dependence of the scattered light intensity makes quantitative evaluation of oligomeric species difficult when polydisperse populations of Aβ exist. Fluorescence resonance energy transfer data were consistent with Aβ existing as a dimer (10, 32), yet the low resolution of this method does not allow determination of the actual oligomer distribution. Solution NMR investigations, in contrast, have not revealed the presence of stable oligomers when the spectroscopy was performed in the absence of fluoroalcohols or detergents (37–40). However, in solution NMR studies of Aβ, the NMR signal decreases and broadens as soon as aggregation begins; thus, no data can be obtained for oligomers.

One approach for stabilizing oligomeric fibril intermediates is chemical cross-linking. Aβ pentamers and hexamers have been observed by SDS-PAGE following glutaraldehyde-mediated cross-linking of Aβ-(1–40) (9), whereas no oligomers were observed without cross-linking. However, glutaraldehyde cross-linking is a method normally used for determination of the subunit structure of oligomeric proteins. Artifacts can be produced when the technique is applied to peptides such as Aβ. For example, nonnative interpeptide interactions resulting from the random collision of peptides may be observed, because the length of the cross-linker is large relative to the size of the peptide. This effect is exacerbated due to the relatively long reaction time required for the cross-linking.

An ideal method for determining Aβ oligomer size distributions would provide accurate, quantitative "snapshots" of the distributions. Because Aβ assembly is a dynamic, multistep process, the method should be applicable within a time interval significantly smaller than the lifetimes of those stages of the fibrillogenesis process to be studied. In addition, in order to accurately reveal the native oligomerization state of Aβ peptide populations, the method should require no prior peptide modification nor the insertion of exogenous cross-linking agents. A method with these characteristics, PICUP (41), has been developed recently. This method enables formation of covalent bonds between closely interacting polypeptide chains without any *pre facto* chemical modifications (*e.g.* introduction of chemically or photochemically reactive moieties into the polypeptide chain) and without using spacers. The PICUP cross-linking reaction is induced by very rapid, visible light photolysis of a tris-bipyridyl Ru(II) complex in the presence of an electron acceptor. Following irradiation, a Ru(III) ion is formed, which serves as an electron abstraction agent to produce a carbon radical within the polypeptide (backbone or side chain), preferentially at positions where stabilization of the radical by hyperconjugation or resonance is favored. The radical reacts very rapidly with a susceptible group in its immediate proximity to form a new C–C bond (a more complete discussion may be found in Refs. 41 and 42). PICUP thus produces a population of oligomers whose oligomerization states have been "frozen" by covalent cross-linking. Analysis of the "frozen" products reveals the state of aggregation that was present just prior to cross-linking. Here we report the use of PICUP to determine the Aβ oligomer distribution existing during the prenucleation phase of fibril assembly.

EXPERIMENTAL PROCEDURES

Peptides and Reagents—Aβ-(1–40) was synthesized using automated Fmoc (9-fluorenylmethoxycarbonyl) chemistry, as previously described (36). The peptide was purified to >97% purity by reverse-phase HPLC and characterized by amino acid analysis and mass spectrometry. Human pituitary adenylate cyclase-activating polypeptide (PACAP), human growth hormone-releasing factor (GRF), and human calcitonin (CT) were purchased from Bachem (Torrance, CA). Human transthyretin (TTR) was kindly provided by Dr. Maria Saraiva (University of Porto, Portugal). Tris(2,2′-bipyridyl)dichlororuthenium(II) (Ru(Bpy)) and ammonium persulfate (APS) were purchased from Aldrich. Polyacrylamide gels, buffers, stains, standards, and equipment for SDS-PAGE were purchased from Invitrogen (Carlsbad, CA). Water was double-distilled and then deionized using a Milli-Q system (Millipore Corp., Bedford, MA). Solvents for HPLC were purchased from Sigma and were of the highest purity available.

Isolation of Low Molecular Weight (LMW) Aβ Peptides and Control Peptides—LMW Aβ-(1–40) was isolated using two methods. For most purposes, SEC was used, as described (13, 22). Briefly, 160 μl of a 2 mg/ml (nominal concentration) peptide solution in Me$_2$SO were sonicated for 1 min using a Branson Ultrasonics bath sonicator (Danbury, CT) and then centrifuged for 10 min at 16,000 × g. The resulting supernate was fractionated on a Superdex 75 HR 10/30 column using 10 mM sodium phosphate buffer, pH 7.4, at a flow rate of 0.5 ml/min. The middle of the LMW peak was collected during 50 s and used immediately for PICUP experiments. A 10-μl aliquot was taken for amino acid analysis to determine quantitatively the peptide concentration in each preparation. Typically, the concentration was 30 ± 3 μM. LMW Aβ was also isolated by filtration through a 10,000 molecular weight cut-off filter (43). Briefly, the peptide was dissolved in water and diluted with 20 mM sodium phosphate buffer, pH 7.4, to a nominal final concentration of 2 mg/ml. Microcon-10 filters (Millipore Corp.) were washed twice with 200 μl of 10 mM sodium phosphate buffer, pH 7.4, prior to sample loading. The peptide solution was sonicated for 1 min and then filtered through the prewashed filter at 16,000 × g during 30 min. The filtrate was used immediately for PICUP. The concentrations of LMW Aβ-(1–40) prepared in this way were somewhat lower (23 ± 3 μM) than those of LMW Aβ-(1–40) isolated by SEC. The volumes taken for SDS-PAGE were adjusted according to the concentration found by amino acid analysis, so that equal amounts of protein were loaded in each lane.

Photochemistry—The photosystem required for performing PICUP experiments was constructed according to the protocol of Fancy and Kodadek (41) with some modifications. Irradiation was accomplished

Amyloid β-Protein Oligomerization

using a 200-watt incandescent lamp (model 170-D; Dolan-Jenner, Lawrence, MA) and a 35-mm Pentax camera body with an attached bellows. The bellows was used to isolate the reaction tube from external light. The lamp was positioned 15 cm from the reaction tube at the open back of the camera. Unless otherwise stated, the irradiation time was 1 s and was controlled precisely using the camera shutter.

Cross-linking of Peptides—In a typical experiment, 1 μl of 1 mM Ru(Bpy) and 1 μl of 20 mM APS in buffer A (10 mM sodium phosphate, pH 7.4) were added to 18 μl of freshly isolated LMW peptide. The mixture was irradiated, and the reaction was quenched immediately with 10 μl of Tricine sample buffer (Invitrogen) containing 5% β-mercaptoethanol. Control peptides were cross-linked under similar conditions.

Cross-linking of Human TTR—Aliquots from a stock solution of TTR (6.5 mg/ml (470 μM) in H₂O) were diluted in either slightly basic buffer (50 mM sodium phosphate, pH 7.5, 100 mM KCl) or acidic buffer (50 mM sodium acetate, pH 3.0, 100 mM KCl, 0.5 mg/ml of the zwitterionic detergent Z 3–14 (Calbiochem) (44)). The samples were incubated for 24 h at 37 °C, and then the protein was cross-linked using 2 μl of 1 mM Ru(Bpy) and 2 μl of 20 mM APS prepared in the same buffer as the protein. The final TTR concentration was 30 μM.

SDS-PAGE and Densitometric Analysis—Samples were analyzed using 1-mm-thick, 10–20% Tris-Tricine gradient gels. Noncross-linked peptide was used as a control for each cross-linked peptide. Peptide bands were visualized by silver staining (SilverXpress, Invitrogen). Gels were air-dried and then scanned with a PowerLook IIIse scanner (Umax, Fremont, CA) in transmissive mode, RGB color, and 600-dot per inch resolution. The scans were saved in TIFF format and imported into One-Dscan (Macintosh version 2.2.4; Scanalytics, Fairfax, VA). The color images were converted to 256 grayscale. A densitometry profile was obtained for each lane, and the relative intensities were calculated by integration of the area under each peak after base-line correction.

RESULTS

Applicability of PICUP to Studies of Aβ Oligomerization—Although PICUP has been used to cross-link proteins whose native states were homo- or heterocomplexes (41, 42, 45), it has not been applied to peptides in the molecular weight range of Aβ. Therefore, a set of cross-linking experiments were carried out to evaluate the utility of the PICUP method for investigating Aβ oligomerization. Particular attention was paid to evaluating the necessity of each of the reaction components and the efficiency of the method. Approximately 0.5 nmol of LMW Aβ-(1–40), freshly isolated by SEC, was irradiated with visible light for 1 s using a ~2-fold molar excess of Ru(Bpy) and ~40-fold molar excess of APS. Control reactions were performed without Aβ, Ru(Bpy), APS, Ru(Bpy) and APS, or light (Fig. 1). In the presence of all reaction components, efficient cross-linking took place, leading to the formation of covalently associated oligomers ranging from dimer through hexamer (*lane 1*). In some cases, the highest observed band was a heptamer. Band intensity differences such as this arose due to differences in the concentration of the LMW Aβ-(1–40) fraction obtained from SEC. Ru(Bpy) and light were required for cross-linking to occur (*lanes 3* and *6*). In the absence of APS, very faint bands corresponding to dimer and trimer were observed (*lane 4*). Under these conditions, cross-linking probably occurs via singlet oxygen as the electron acceptor (46, 47), albeit with a much lower efficiency (41, 45). The fact that no oligomers were detected without irradiation rules out the possibility of observing noncovalent Aβ-(1–40) oligomers that either are not dissociated or are induced in the presence of SDS. Theoretically, the cross-linked oligomers could serve as nuclei for aggregation of free monomers and therefore skew the distribution observed by SDS-PAGE. However, boiling the samples for 10 min with sample buffer containing 8 M urea did not have an effect on the numbers or relative intensities of oligomers observed (data not shown). Thus, the observed bands represent only covalently associated oligomers.

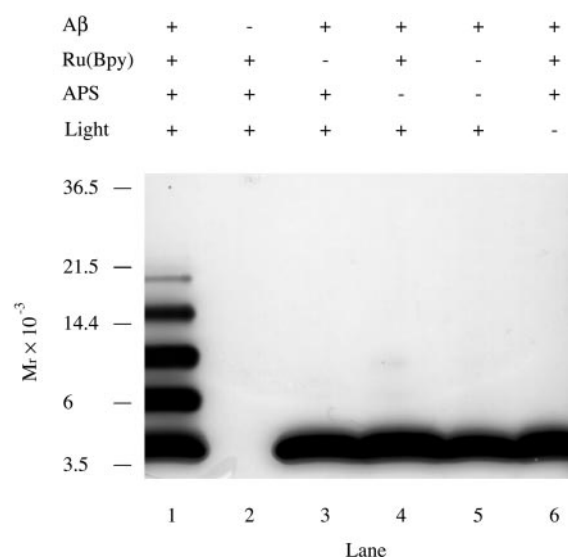*Effect of the Method of LMW Aβ Isolation on Cross-linking*—Theoretically, if oligomers were in rapid equilibrium with

FIG. 1. **SDS-PAGE of Aβ-(1–40) following PICUP chemistry.** LMW Aβ was subjected to the PICUP reaction, and the resulting products were analyzed by SDS-PAGE on a 10–20% gradient gel. Bands were visualized using silver staining. *Lane 1*, Aβ plus all reactants. *Lanes 2–6*, control reactions performed without Aβ, Ru(Bpy), APS, Ru(Bpy) and APS, or light. The mobilities of molecular weight markers are shown on the *left*. The gel is representative of each of five independent experiments.

monomers, SEC could produce a singlet LMW Aβ peak that contained both monomers and small oligomers and displayed an aberrant retention time. In fact, the retention times observed for LMW Aβ can vary significantly depending on gel and solvent composition (13). In sodium phosphate buffer, retention times most often correspond to those of a dimer or trimer rather than a monomer (13). To determine whether the SEC fractionation of Aβ indeed produced a homogeneous LMW Aβ population, we examined an alternative preparation method, filtration through membranes of 10,000 MWCO. These membranes retain Aβ species larger than a dimer (MW ≈ 8660). If the lifetimes of any small oligomers were long, only monomers and dimers would pass through the filter membrane. On the other hand, if oligomers were in rapid equilibrium with monomers or dimers, once the monomers and dimers in the Aβ preparation had passed through the membrane, the remaining oligomers would quickly dissociate (according to Le Châtelier's principle (48, 49)), leading to passage of the majority of the peptide through the membrane. In the former case, cross-linking should yield mainly monomers and dimers, whereas in the latter case, a distribution would be observed similar to that of SEC-isolated Aβ.

LMW Aβ-(1–40) was isolated both by SEC and filtration and was cross-linked as described above. The distributions of cross-linked oligomers observed in each case were highly similar (Fig. 2), both with regard to the total number of oligomers and to their relative intensities. These results strongly suggest that "LMW" Aβ-(1–40) is, in fact, a mixture of small oligomers undergoing rapid association and dissociation during SEC, precluding resolution of individual components.

PICUP Analysis of Amyloidogenic and Nonamyloidogenic Control Peptides—The distribution of oligomers observed for Aβ-(1–40) indicated that a population of small oligomers existed in rapid equilibrium with monomer. This distribution may be unique to Aβ and related to the aggregation propensity of the peptide. Alternatively, the distribution may result from the random collision of molecules diffusing in solution. To distinguish between these possibilities, experiments were conducted using another amyloidogenic peptide, human calcitonin
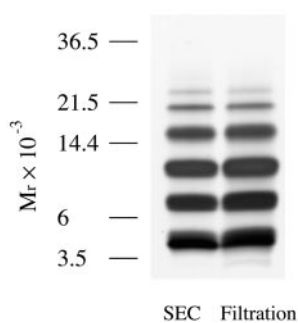
FIG. 2. **Effects of preparation method on cross-linking.** LMW Aβ-(1–40) was isolated either by SEC or by filtration through a 10,000 MWCO filter. PICUP reactions were performed immediately, and then the products were analyzed by SDS-PAGE. The mobilities of molecular mass markers are shown on the *left*. The gel is representative of each of three independent experiments.

(MW = 3418), and two nonamyloidogenic peptides, human pituitary adenylate cyclase-activating polypeptide (MW = 4534) and human growth hormone-releasing factor (MW = 5040). The molecular weight of each peptide is similar to that of Aβ-(1–40) (MW = 4330).

As mentioned above, Aβ-(1–40) chromatographs aberrantly, producing an apparent retention time equivalent to that of a dimer or a trimer. In fact, it is this peculiar behavior that enables the isolation of the LMW Aβ fraction. Under the same conditions, PACAP and GRF migrated as monomers that could not be resolved from the Me$_2$SO solvent peak. Therefore, for all peptides, filtration was used in this experiment rather than SEC. PACAP, GRF, and CT were dissolved in 10 mM sodium phosphate, pH 7.4, and filtered through a 10,000 MWCO membrane, in the same manner as Aβ-(1–40), to ensure that the preparations did not contain preformed aggregates. Following cross-linking, the distributions of cross-linked oligomers of the four peptides were determined by SDS-PAGE (Fig. 3*A*). In order to estimate the relative abundance of each oligomer, each lane was scanned and quantified. Fig. 3, *B–E*, shows the averaged oligomer distributions from six independent experiments.

The oligomer distributions obtained for the two nonamyloidogenic peptides were distinct from those of the amyloidogenic peptides. PACAP and GRF yielded continuous oligomer distributions ranging from dimer through dodecamer (Fig. 3, *A*, *C*, and *D*). On average, in both cases, dimers were the most abundant species, and the relative amounts of the other oligomers decreased exponentially with increasing molecular weight. Monomers were also present in each case, although the PACAP monomer was not observed in all experiments. Electrophoretic analysis of these peptides without cross-linking revealed that noncross-linked GRF produced only a monomer band, whereas noncross-linked PACAP showed a predominant dimer band (data not shown). Accordingly, the cross-linked PACAP distribution contained very little monomer. The highest oligomers observed for the two nonamyloidogenic peptides had apparent molecular masses of 55–60 kDa. In contrast, the cross-linked amyloidogenic peptides, Aβ-(1–40) and CT, displayed oligomer distributions extending only to heptamer or hexamer, respectively. Aβ-(1–40) produced a continuous oligomer distribution in which the abundances of species ranging from monomer through tetramer diverged significantly from an exponential curve. The heptamer band was not observed in all cases. CT displayed a noncontinuous profile that strongly diverted from an exponential curve in the region monomer through tetramer. An exponential decrease of the relative oligomer abundances was observed only in the higher molecular weight regimes for both Aβ-(1–40) and CT. Here, the magnitude of the exponential was high, creating a sharp molecular weight-dependent de-
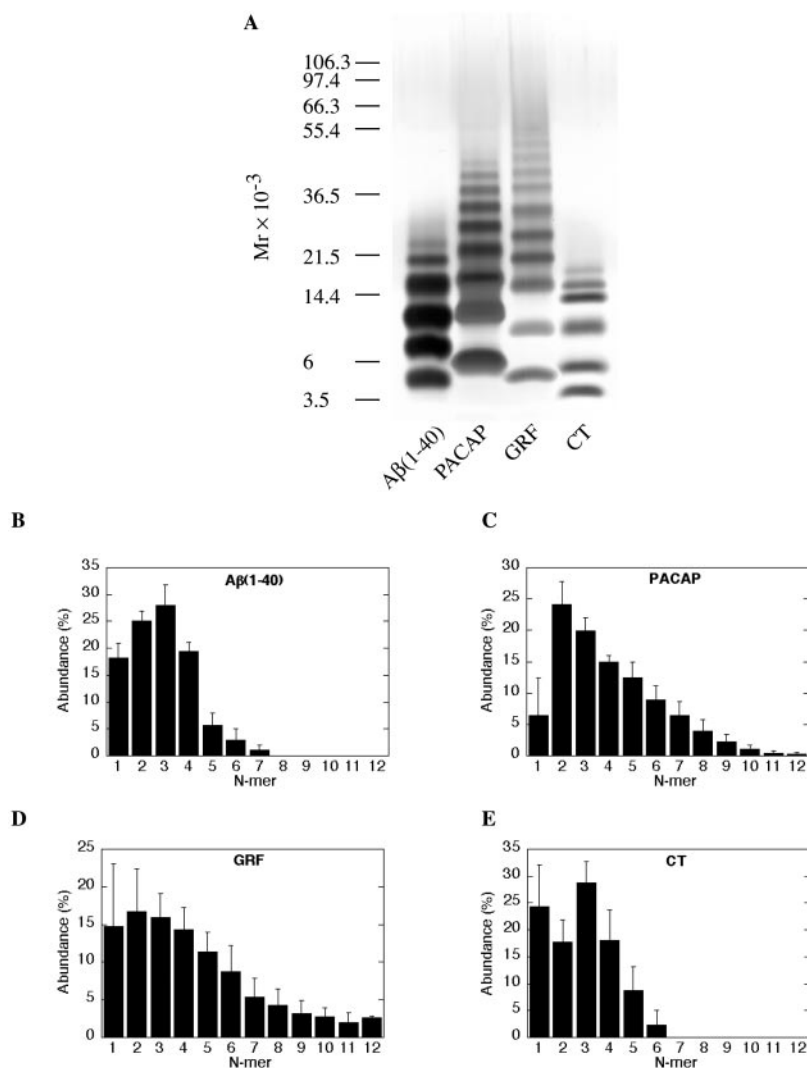
cline in oligomer abundance, in contrast to the shallower exponential curves observed for PACAP and GRF. The molecular masses of the highest bands observed in the Aβ and CT samples were ~26 and ~18 kDa, respectively. In conclusion, distinct oligomer distributions were found for the nonamyloidogenic peptides, PACAP and GRF, compared with the amyloidogenic peptides, Aβ-(1–40) and CT.

PICUP Analysis of TTR—To further investigate whether the apparent differences between the amyloidogenic and the nonamyloidogenic peptides correlated with their aggregation properties or reflected merely arbitrary composition and/or sequence differences, PICUP was performed on TTR, a protein associated with familial amyloid polyneuropathy and senile systemic amyloidosis (50). TTR normally exists as a stable tetramer; however, under appropriate conditions, it can dissociate into a monomer and can form amyloid fibrils. Based on the results obtained for the amyloidogenic and nonamyloidogenic peptides, we predicted that cross-linking the monomer should yield a "ladder" of oligomers displaying an exponential decrease of abundances, whereas the tetramer should give rise to a limited distribution of oligomers, each composed of an integer number of tetramers.

TTR was incubated for 24 h at 37 °C either at pH 3.0, in the presence of the zwitterionic detergent Z 3–14, or at pH 7.5, in the absence of Z 3–14. Because the TTR tetramer is highly resistant to dissociation (44, 51, 52), extended incubation (24 h) under acidic conditions was required to produce substantial amounts of monomer. In addition, the monomers had to be stabilized to prevent their assembly into fibrils. This was accomplished by the addition of Z 3–14 (51). Following incubation, the protein was cross-linked, and the products were diluted with reducing sample buffer, boiled for 10 min, and analyzed by SDS-PAGE. As has been shown previously (44, 52), without cross-linking, monomer and dimer bands predominated at both pH 7.5 and 3.0 (Fig. 4, *lanes 1* and *3*, respectively). A very faint tetramer band, representing <0.5% of the total TTR protein, was observed in some of the experiments at pH 7.5 (data not shown). TTR incubated at pH 3.0 apparently refolds and forms dimers rapidly upon dilution in SDS sample buffer (which brings the pH to ~9 and disrupts the Z 3–14 micelles), since essentially the same profile was obtained for the noncross-linked TTR both at pH 3.0 and 7.5. As predicted, cross-linking of TTR preincubated at pH 3.0 yielded a "ladder" of oligomers ranging from monomer through nonamer (Fig. 4, *A* (*lane 4*) and *C*), consistent with the protein dissociating into monomer due to the acid treatment. In contrast, at pH 7.5, TTR yielded mainly monomer and dimer (Fig. 4, *A* (*lane 2*) and *B*). Under this condition, the dimer population was enriched ~2-fold relative to the noncross-linked TTR. In addition to monomer and dimer bands, cross-linking of TTR at pH 7.5 produced three bands of higher molecular mass (Fig. 4*A* (*lane 2*)), the slowest migrating of which displayed the same mobility as did the native TTR tetramer (data not shown). This result suggests that the TTR tetramer maintains its overall compact structure following cross-linking and therefore migrates faster than would be predicted by its molecular weight. The two other bands presumably represent different cross-linked forms of TTR with similar molecular masses but different mobilities.

The overall yield of intermolecularly cross-linked TTR at pH 7.5 was considerably lower (only ~50% conversion of monomer) than that obtained at pH 3.0 (~80% conversion of monomer). The quaternary structure of TTR thus may facilitate intramolecular or dimer cross-linking and significantly limit the extent to which higher cross-linked oligomers are formed, presumably due to unfavorable orientation of reactive side chains (*e.g.* Tyr or Trp (45)). The crystal structure of TTR complexed with a

Amyloid β-Protein Oligomerization

A

FIG. 3. **PICUP analysis of amyloidogenic and nonamyloidogenic peptides.** Aβ-(1–40), PACAP, GRF, and CT were filtered through 10,000 MWCO filters and then immediately subjected to PICUP. The products were resolved by SDS-PAGE and silver staining (*A*) and quantified by densitometric analysis (*B–E*). The mobilities of molecular mass markers are shown to the *left* of *A*. The gel is representative of results obtained in each of six independent experiments. *B–E* show the averaged distributions observed in these six experiments. Some variation among experiments was observed due to concentration differences following filtration. The variation was most pronounced for low order oligomers of PACAP and GRF. In addition, the low order oligomers of these two peptides displayed some heterogeneity in their staining. For example, although the PACAP monomer is not observed in *A*, it was apparent in other experiments. In addition, irregular migration of some of the small oligomers of the control peptides caused certain bands to appear wide and more diffuse, while others were narrow and sharp.

fibrillogenesis inhibitor that stabilizes the native structure of the protein reveals that the majority of the reactive groups (such as Tyr and Trp) are either buried in the hydrophobic core of each monomer or at the "dimer interface" (53). This result is in agreement with the propensity of the protein to produce mainly "within dimer" or intramolecular cross-linking. This burial of reactive groups also accounts for the lack of oligomers higher than tetramers observed following cross-linking of native TTR. Nevertheless, these results demonstrate that PICUP is capable of distinguishing between monomeric and oligomeric states of the same protein, since the relative oligomer distributions obtained in each case were very distinct.

Effect of Irradiation Time on Aβ-(1–40) PICUP Products—To further evaluate the genesis of the unique oligomer distribution observed for Aβ-(1–40), the effect of irradiation time was examined. LMW Aβ-(1–40) was cross-linked with irradiation times ranging from 1/30 to 60 s (Fig. 5). In agreement with our previous observations, which suggested an equilibrium among monomer, dimer, trimer, and tetramer, substantial amounts of dimer, trimer, and tetramer, but only trace amounts of pentamer and no higher oligomers, were observed even at the shortest exposure time (Fig. 5*A*). At longer exposure times, up to 8 s, the apparent abundances of all oligomers increased. To determine the effect of irradiation time on the *relative* abundance of each oligomer, densitometric analysis was performed. In this process, the intensity of each oligomer at a particular irradiation time was normalized relative to the sum of all intensities

in the lane (Fig. 5*B*). This analysis revealed that the relative abundances of the three smallest oligomers (mainly dimer and tetramer) were initially sensitive to the exposure time. At short exposures, between 1/30 and 1/4 s, as exposure time increases, the relative abundance of dimer decreases somewhat, whereas those of trimer, and especially tetramer, increased. By irradiation times of 1/2 to 1 s, the relative abundances of trimer and tetramer plateaued at values of 24 and 17%, respectively. Longer irradiation times had relatively little effect on these abundances. These observations are consistent with a system in equilibrium, in which perturbations in the concentrations of one or more components are compensated for by equivalent, but opposite, concentration changes in other components, according to Le Châtelier's principle (48, 49). The relative abundance of dimer plateaued in the time regime of 2–8 s but decreased again at longer irradiation times (15–60 s), consistent with the exhaustion of its precursor monomers. At all time points, the abundances of oligomers higher than tetramer displayed an exponential decrease similar to that observed at 1 s of irradiation (densitometry data not shown). However, at higher exposure times, oligomers higher than a heptamer were observed (octamer at 2 s, nonamer at 8 s), and the bands became considerably smeared. The smearing was probably caused by formation of multiple species (intra- and intermolecularly crosslinked) with similar molecular masses but slightly different mobilities in SDS-PAGE. In addition, at higher exposure times, substantial degradation was observed due to the prolonged
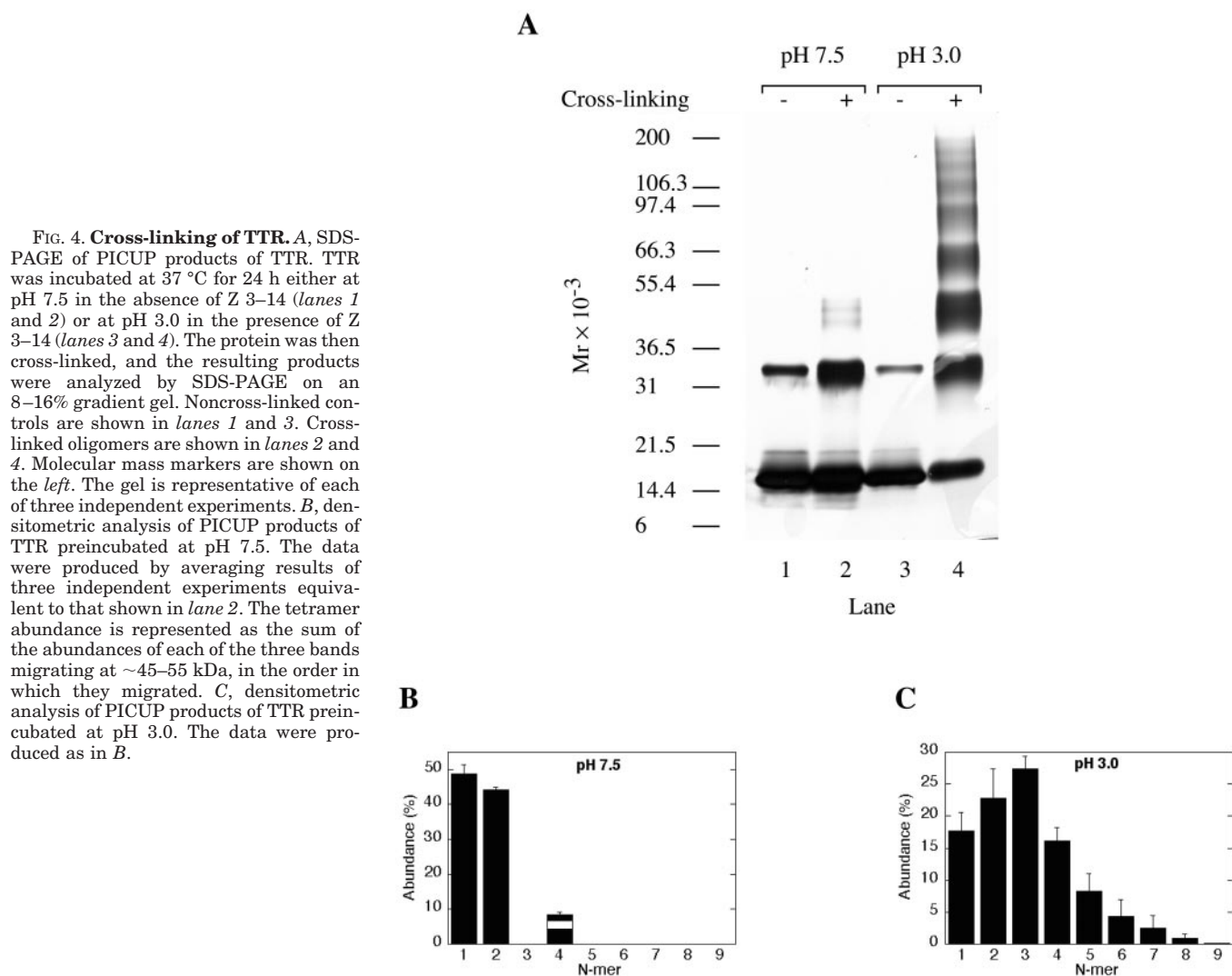
A

FIG. 4. **Cross-linking of TTR.** *A*, SDS-PAGE of PICUP products of TTR. TTR was incubated at 37 °C for 24 h either at pH 7.5 in the absence of Z 3–14 (*lanes 1 and 2*) or at pH 3.0 in the presence of Z 3–14 (*lanes 3 and 4*). The protein was then cross-linked, and the resulting products were analyzed by SDS-PAGE on an 8–16% gradient gel. Noncross-linked controls are shown in *lanes 1 and 3*. Cross-linked oligomers are shown in *lanes 2 and 4*. Molecular mass markers are shown on the *left*. The gel is representative of each of three independent experiments. *B*, densitometric analysis of PICUP products of TTR preincubated at pH 7.5. The data were produced by averaging results of three independent experiments equivalent to that shown in *lane 2*. The tetramer abundance is represented as the sum of the abundances of each of the three bands migrating at ~45–55 kDa, in the order in which they migrated. *C*, densitometric analysis of PICUP products of TTR preincubated at pH 3.0. The data were produced as in *B*.

B

C

radical reaction. Thus, cleavage products (bands lower than monomer) were detected at irradiation times longer than ¼ s, and eventually fading out of the entire lane was observed at 30 and 60 s. Notably, even at these long exposure times, the highest molecular mass observed did not exceed ~50 kDa, in contrast to the distributions observed for the nonamyloidogenic peptides at irradiation times as short as 1 s (Fig. 3).

DISCUSSION

Small oligomers of Aβ are believed to have a direct role in AD pathology, both due to their direct short and long term neurotoxic effects and their ability to give rise to fibrillar assemblies (5). Studies of Aβ oligomerization have suggested that several distinct species are associated with fibril formation (54, 55). However, accurate identification and quantification of these oligomers has been difficult. Here, small, metastable oligomers of unmodified Aβ have been trapped by rapid photochemical cross-linking (PICUP), and their relative abundances have been quantified by SDS-PAGE and densitometry, allowing conclusions to be made about the assembly state of "nascent" Aβ and its early associative interactions.

Analysis of the distributions of Aβ oligomers requires an understanding of the relationship between the cross-linking chemistry and the resulting distribution of oligomers. This understanding is best achieved through the use of simple mathematical models describing a single-substrate cross-linking system. A simple model cannot account for all aspects of a dynamic process such as Aβ fibril assembly. However, if the assumptions of the model are reasonable and the key factors controlling the assembly process are incorporated into the model, valuable insights can be achieved. In the following model, it is assumed that the substrate molecules are monomeric spheres and that the only interaction among them is random elastic collision. As radicals form following irradiation *in vitro* or by initiating a simulation, these collisions occasionally result in the formation of a covalent bond between monomers (*M*), yielding a dimer (*D*),

$$M + M \rightarrow D \qquad (\text{Eq. 1})$$

The reaction is irreversible, and if no other reactions take place, the rate of monomer consumption is equal to twice that of dimer formation,

$$-\frac{d[M]}{dt} = 2\frac{d[D]}{dt} = k_{1,1}[M]^2 \qquad (\text{Eq. 2})$$

The efficiency of the cross-linking reaction (*i.e.* the number of dimers produced per unit time) is characterized by the rate constant, $k_{1,1}$. The dimers that have been formed may further react with monomers to form trimers or with other dimers to form tetramers. These products in turn react further to produce oligomers of increasing order. Because reactions of third or higher orders are extremely rare, it is assumed in this model that all of the products are formed only by bimolecular reac-
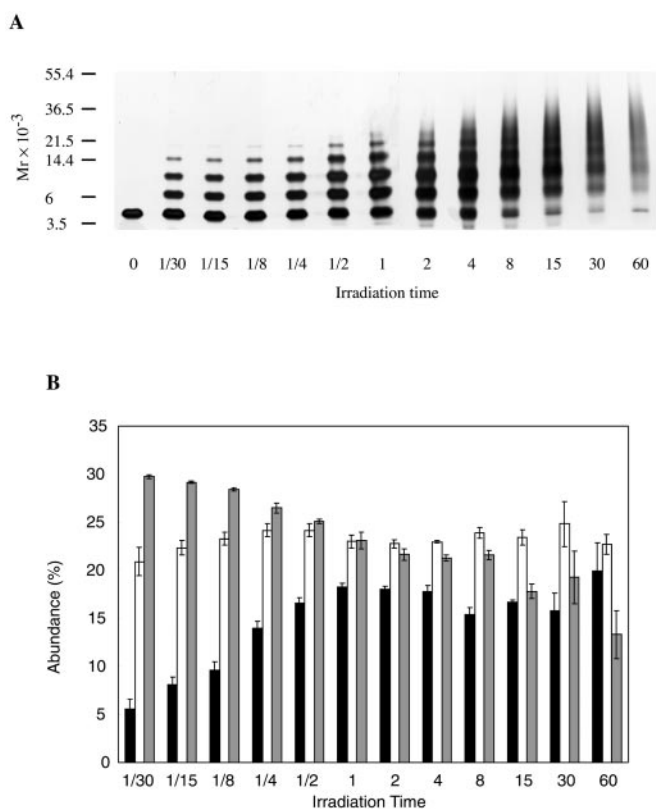
FIG. 5. **Effects of irradiation time on Aβ-(1–40) oligomer distributions.** *A*, SDS-PAGE of PICUP reactions performed with irradiation times between ⅟₃₀ and 60 s. Molecular mass markers are shown on the *left*. The gel is representative of each of three independent experiments. *B*, quantitative analysis of the relative abundances of the dimer, trimer, and tetramer species as a function of the irradiation time. The abundance of each oligomer is normalized relative to the whole lane. The graph represents average values of three independent experiments. *Black*, tetramer; *white*, trimer; *hatched*, dimer.

tions, and therefore only second order reactions are taken into account. The formation of oligomers of the *n*th order, X_n, is described by Equation 3,

$$X_i + X_{n-i} \rightarrow X_n \qquad \text{(Eq. 3)}$$

for $i = 1$ to $n - 1$. Because X_n is further consumed to form larger oligomers, the concentration of X_n changes with time according to the system of Equation 4.

$$\frac{d[X_n]}{dt} = \sum_{i=1}^{n-1} k_{i,n-i}[X_i][X_{n-i}] - \sum_{i=1}^{\infty} k_{i,n}[X_i][X_n] \qquad \text{(Eq. 4)}$$

Integration of Equation 4 over time yields the distribution of oligomers at any time point during the reaction. In this model, if only monomers are present at the beginning of the reaction simulation, the observed distribution of cross-linked oligomers (X_n) at a given time point is a function of the initial monomer concentration and the cross-linking rate constants $k_{i,n}$. By numerical integration of Equation 4, a series of theoretical oligomer distributions may be generated (Fig. 6). Since no data are available for the cross-linking rate constants of the different oligomers, an identical constant was assigned to all of the reactions. This approximation is reasonable because, although cross-linking efficiency increases with oligomer size due to the availability of more reactive sites per molecule, the likelihood of cross-linking decreases because the diffusion coefficients of the larger oligomers make their interaction with other oligomers less probable. It is important to note that this model does not seek to account for every aspect of the highly complex

process of protein cross-linking by PICUP. Rather, we have sought to formulate a simple mathematical model incorporating conservative assumptions in order to conceptualize the principal relationships between the chemistry used and the observed results.

Fig. 6 illustrates three representative distributions obtained by simulating the cross-linking reaction for a given time while changing the reaction rate constant. When cross-linking efficiency is low, few oligomers are formed, and the reaction mixture contains mainly unreacted monomer (Fig. 6*A*). The observed distribution of species mimics a steeply decreasing exponential function. As efficiency increases, larger oligomers are observed and the distribution resembles a more slowly decreasing exponential (Fig. 6*B*). When the efficiency is high, monomers are rapidly consumed in the formation of dimers and higher oligomers. Accordingly, the maximum of the distribution may shift from the monomer to higher order oligomers and the shape resembles an asymmetric Gaussian function (Fig. 6*C*).
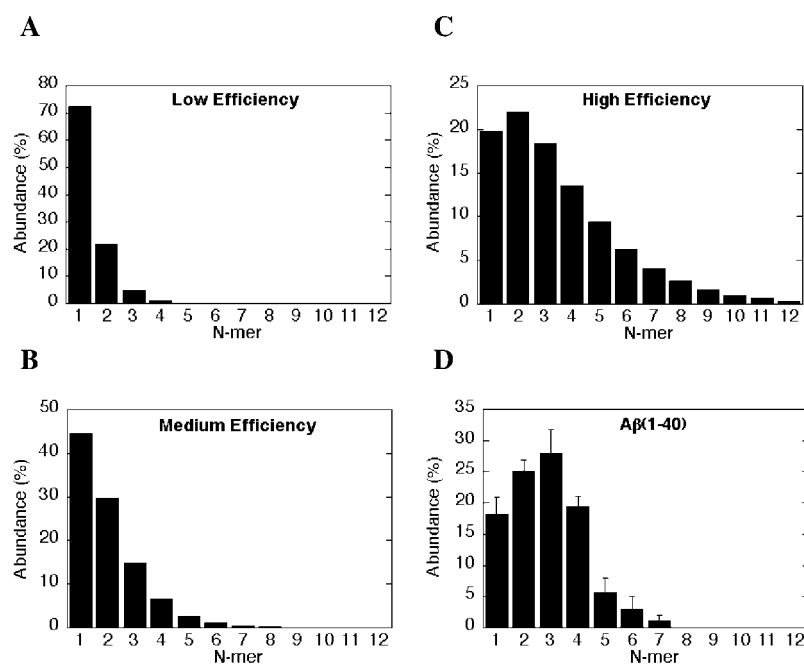
The results obtained in our PICUP experiments may be divided into three groups, classified by the numbers and relative abundances of the oligomers produced. The first group is characterized by a high number (~10 or more) of apparent oligomers whose abundances decrease nearly exponentially. The maximum of the distribution may be monomer, dimer, or trimer, and the overall shape is similar to the theoretical distributions in Fig. 6, *B* or *C*. This type of distribution was obtained for the nonamyloidogenic peptides GRF and PACAP (Figs. 3, *C* and *D*, respectively) and for the monomeric form of TTR (Fig. 4*C*). A similar profile was observed for monomeric lysozyme (45). This group therefore represents a system of nonassociating monomers with high cross-linking efficiency.

The second group is characterized by two features, an irregular shape in the low order oligomer region (monomer through tetramer) and a steep exponential decrease of abundances of oligomers above tetramer, ending at hexamer or heptamer. The maximum of the distribution is within the irregular region. This type of distribution was observed for the amyloidogenic peptides Aβ-(1–40) and CT. The irregular region strongly departs from the theoretical distributions calculated by the model, which assumes that only monomers are present initially. Therefore, this type of distribution cannot represent a system of nonassociating molecules and more likely reflects the preassociation of small oligomers. This association minimizes diffusion-associated, "nonspecific" cross-linking of monomers. Cross-linking efficiency is maintained at a high level, but the distribution is markedly biased in favor of the preassociated oligomers. We note, however, based on the results of the filtration experiment (Fig. 2), that unlike stable, multimeric proteins, the Aβ oligomers are in rapid equilibrium.

The third group includes stable, multimeric proteins such as the native TTR tetramer or proteins observed in other PICUP studies, including glutathione *S*-transferase, ecotin, and the yeast transcription factor Pho4 (45). This group is characterized by a limited distribution of oligomers, which represents mainly the oligomerization state of the proteins themselves.

As in any experimental system, PICUP is not free from systematic errors and "noise." One type of "noise," which mostly affects the preassociated peptide group, is caused by free monomer, which can still react in a random manner either with other monomers or with the preassociated oligomers. This random component produces an exponential "tail" of oligomers larger than those that are in equilibrium. Thus, the equilibrium mixture is likely to include only those oligomers that clearly diverge from the exponential part of the curve. In the case of Aβ-(1–40) and CT, these species are monomer through

A

C

B

D

FIG. 6. **Simulated distributions of PICUP-generated oligomers produced from nonassociating molecules in solution.** These distributions are derived from a mathematical model, which assumes free diffusion of spherical molecules and a fixed concentration of starting monomer. The resulting oligomer distributions are a function of the cross-linking efficiency: low efficiency (*A*), medium efficiency (*B*), and high efficiency (*C*). D, the distribution observed for Aβ-(1–40) is presented for comparison.

tetramer. A second intrinsic experimental bias in the PICUP system, which again affects mostly the preassociated peptide group, results from the cross-linking efficiency being <100%. As a result, the apparent abundances observed by SDS-PAGE represent a distribution that is shifted toward smaller oligomers relative to the real distribution of preassociated oligomers in the sample. For example, in a dimer, one cross-link between the two chains is sufficient for the pair to appear as a dimer on a gel. In a trimer, on the other hand, at least two intermolecular cross-links that involve all three chains must be formed in order for the trimer to appear as such on a gel. If one chain fails to cross-link to at least one of the other two, the apparent result will not be a trimer but rather a monomer and a dimer. This bias is most pronounced at short exposure times, as shown in Fig. 5. However, with a sufficiently long irradiation time, this effect becomes less significant, and the mean values observed for dimer, trimer, and tetramer between ½ and 15 s of exposure (before excessive degradation occurs) are likely to represent the actual abundances, within experimental error, prior to cross-linking.

LeVine has also examined the quaternary state of Aβ in solution (9). To do so, glutaraldehyde-mediated chemical cross-linking was used to stabilize complexes prior to gel electrophoresis. Depending on the precise experimental conditions used, this approach generally revealed distributions of oligomers ranging from monomer through heptamer. The distributions exhibited monotonic decreases in "oligomer" abundance, beginning with monomer. Analysis of these data led LeVine to propose a model of fibril formation involving a monomer [dharrow] pentamer/hexamer equilibrium and the assembly of the pentamer/hexamer unit into fibrils. Our results also suggest that prenucleation phases of Aβ fibrillogenesis involve monomer [dharrow] oligomer equilibria. However, recent advances in methods for isolation of LMW Aβ and in cross-linking chemistry (PICUP) allowed us to obtain significant new insights. The data suggest that the equilibria involve primarily monomer, dimer, trimer, and tetramer. It is likely that technical differences in the two approaches are responsible for the differing conclusions. The glutaraldehyde chemistry required that the cross-linking reaction be performed at pH 6, close to the isoelectric point of Aβ, where peptide aggregation is facilitated. In order to reduce aggregation, Aβ was treated with

1,1,1,3,3,3-hexafluro-2-propanol prior to cross-linking. However, moderate concentrations of fluoroalcohols can accelerate fibrillogenesis, as shown for acylphosphatase (56) and Aβ[2] in the presence of trifluoroethanol. Thus, the experimental conditions used in the glutaraldehyde cross-linking study may have promoted aggregation of Aβ, shifting the oligomer distribution to higher order. In addition, because the glutaraldehyde cross-linking chemistry required extended incubation time (2–10 min), substantial random cross-linking could occur, leading to the production of oligomers larger than those that actually existed at the initiation of the cross-linking reaction. In contrast, the PICUP reaction was done at physiologic pH, in the absence of organic modifiers, and with a short incubation time (1 s). Thus, the oligomer frequency distribution produced using PICUP is likely to accurately reflect the preexisting oligomer composition of LMW Aβ. Further, these data demonstrate that a dynamic process of oligomer formation and dissociation precedes Aβ aggregation, suggesting that Aβ fibrillogenesis follows a more complex pathway than that suggested by simple two-step nucleation-elongation models.

In summary, we have demonstrated that small Aβ oligomers can be efficiently cross-linked by PICUP. By taking "snapshots" of the oligomer size distributions of Aβ and comparing them with those of other amyloidogenic and nonamyloidogenic peptides, important questions of biological relevance can be answered. Here we addressed the question of the oligomerization state of LMW Aβ, an issue for which no consensus had yet been achieved. Our data revealed that LMW Aβ-(1–40) is, in fact, a population of monomer, dimer, trimer, and tetramer in rapid equilibrium. In addition, the distinct oligomer size distributions found for the amyloidogenic and nonamyloidogenic peptides studied here suggest that PICUP may be a useful tool for distinguishing between these two types of peptides and for identifying conditions under which benign peptides may become amyloidogenic. The technique may also be used for probing the structural factors that control the early steps of Aβ aggregation. For example, PICUP has been used to determine the effects of structural modifications at the N terminus, midregion, and C terminus of Aβ on the oligomer size distribu-

---

[2] Y. Fezoui and D. B. Teplow, manuscript in preparation.

tion.[3] These latter studies provide mechanistic insights into the pathologic behavior of Aβ peptides associated with clinically relevant AβPP mutations.

REFERENCES

1. Selkoe, D. J. (1991) *Neuron* **6**, 487–498
2. Teplow, D. B. (1998) *Amyloid: Int. J. Exp. Clin. Invest.* **5**, 121–142
3. Selkoe, D. J., Yamazaki, T., Citron, M., Podlisny, M. B., Koo, E. H., Teplow, D. B., and Haass, C. (1996) *Ann. N. Y. Acad. Sci.* **777**, 57–64
4. Selkoe, D. J. (1999) *Nature* **399**, (suppl.) A23–A31
5. Klein, W. L., Krafft, G. A., and Finch, C. E. (2001) *Trends Neurosci.* **24**, 219–224
6. Scherzinger, E., Lurz, R., Turmaine, M., Mangiarini, L., Hollenbach, B., Hasenbank, R., Bates, G. P., Davies, S. W., Lehrach, H., and Wanker, E. E. (1997) *Cell* **90**, 549–558
7. Conway, K. A., Lee, S. J., Rochet, J. C., Ding, T. T., Williamson, R. E., and Lansbury, P. T. (2000) *Proc. Natl. Acad. Sci. U. S. A.* **97**, 571–576
8. Roher, A. E., Chaney, M. O., Kuo, Y. M., Webster, S. D., Stine, W. B., Haverkamp, L. J., Woods, A. S., Cotter, R. J., Tuohy, J. M., Krafft, G. A., Bonnell, B. S., and Emmerling, M. R. (1996) *J. Biol. Chem.* **271**, 20631–20635
9. LeVine, H., III (1995) *Neurobiol. Aging* **16**, 755–764
10. Garzon-Rodriguez, W., Sepulveda-Becerra, M., Milton, S., and Glabe, C. G. (1997) *J. Biol. Chem.* **272**, 21037–21044
11. Lambert, M. P., Barlow, A. K., Chromy, B. A., Edwards, C., Freed, R., Liosatos, M., Morgan, T. E., Rozovsky, I., Trommer, B., Viola, K. L., Wals, P., Zhang, C., Finch, C. E., Krafft, G. A., and Klein, W. L. (1998) *Proc. Natl. Acad. Sci. U. S. A.* **95**, 6448–6453
12. Harper, J. D., Wong, S. S., Lieber, C. M., and Lansbury, P. T. (1997) *Chem. Biol.* **4**, 119–125
13. Walsh, D. M., Lomakin, A., Benedek, G. B., Condron, M. M., and Teplow, D. B. (1997) *J. Biol. Chem.* **272**, 22364–22372
14. Kim, S. H., Wang, R., Gordon, D. J., Bass, J., Steiner, D. F., Lynn, D. G., Thinakaran, G., Meredith, S. C., and Sisodia, S. S. (1999) *Nat. Neurosci.* **2**, 984–988
15. Chiti, F., Webster, P., Taddei, N., Clark, A., Stefani, M., Ramponi, G., and Dobson, C. M. (1999) *Proc. Natl. Acad. Sci. U. S. A.* **96**, 3590–3594
16. Conway, K. A., Harper, J. D., and Lansbury, P. T. (1998) *Nat. Med.* **4**, 1318–1320
17. Wilkins, D. K., Dobson, C. M., and Gross, M. (2000) *Eur. J. Biochem.* **267**, 2609–2616
18. Goda, S., Takano, K., Yamagata, Y., Nagata, R., Akutsu, H., Maki, S., Namba, K., and Yutani, K. (2000) *Protein Sci.* **9**, 369–375
19. Yutani, K., Takayama, C., Goda, S., Yamagata, Y., Maki, S., Namba, K., Tsunasawa, S., and Ogasahara, K. (2000) *Biochemistry* **39**, 2769–2777
20. Lashuel, H. A., Lai, Z., and Kelly, J. W. (1998) *Biochemistry* **37**, 17851–17864
21. Ionescu-Zanetti, C., Khurana, R., Gillespie, J. R., Petrick, J. S., Trabachino, L. C., Minert, L. J., Carter, S. A., and Fink, A. L. (1999) *Proc. Natl. Acad. Sci. U. S. A.* **96**, 13175–13179
22. Walsh, D. M., Hartley, D. M., Kusumoto, Y., Fezoui, Y., Condron, M. M., Lomakin, A., Benedek, G. B., Selkoe, D. J., and Teplow, D. B. (1999) *J. Biol. Chem.* **274**, 25945–25952
23. Harper, J. D., Wong, S. S., Lieber, C. M., and Lansbury, P. T. (1999) *Biochemistry* **38**, 8972–8980
24. Hilbich, C., Kisters-Woike, B., Reed, J., Masters, C. L., and Beyreuther, K. (1992) *J. Mol. Biol.* **228**, 460–473
25. Soreghan, B., Kosmoski, J., and Glabe, C. (1994) *J. Biol. Chem.* **269**, 28551–28554
26. Kuo, Y. M., Emmerling, M. R., Vigo-Pelfrey, C., Kasunic, T. C., Kirkpatrick, J. B., Murdoch, G. H., Ball, M. J., and Roher, A. E. (1996) *J. Biol. Chem.* **271**, 4077–4081
27. Pitschke, M., Prior, R., Haupt, M., and Riesner, D. (1998) *Nat. Med.* **4**, 832–834
28. Podlisny, M. B., Ostaszewski, B. L., Squazzo, S. L., Koo, E. H., Rydell, R. E., Teplow, D. B., and Selkoe, D. J. (1995) *J. Biol. Chem.* **270**, 9564–9570
29. Podlisny, M. B., Walsh, D. M., Amarante, P., Ostaszewski, B. L., Stimson, E. R., Maggio, J. E., Teplow, D. B., and Selkoe, D. J. (1998) *Biochemistry* **37**, 3602–3611
30. Xia, W. M., Zhang, J. M., Kholodenko, D., Citron, M., Podlisny, M. B., Teplow, D. B., Haass, C., Seubert, P., Koo, E. H., and Selkoe, D. J. (1997) *J. Biol. Chem.* **272**, 7977–7982
31. Walsh, D. M., Tseng, B. P., Rydell, R. E., Podlisny, M. B., and Selkoe, D. J. (2000) *Biochemistry* **39**, 10831–10839
32. Huang, T. H., Yang, D. S., Plaskos, N. P., Go, S., Yip, C. M., Fraser, P. E., and Chakrabartty, A. (2000) *J. Mol. Biol.* **297**, 73–87
33. Joachim, C. L., Duffy, L. K., Morris, J. H., and Selkoe, D. J. (1988) *Brain Res.* **474**, 100–111
34. McKinley, M. P., and Prusiner, S. B. (1986) *Int. Rev. Neurobiol.* **28**, 1–57
35. Ward, R. V., Jennings, K. H., Jepras, R., Neville, W., Owen, D. E., Hawkins, J., Christie, G., Davis, J. B., George, A., Karran, E. H., and Howlett, D. R. (2000) *Biochem. J.* **348**, 137–144
36. Lomakin, A., Chung, D. S., Benedek, G. B., Kirschner, D. A., and Teplow, D. B. (1996) *Proc. Natl. Acad. Sci. U. S. A.* **93**, 1125–1129
37. Lee, J. P., Stimson, E. R., Ghilardi, J. R., Mantyh, P. W., Lu, Y. A., Felix, A. M., Llanos, W., Behbin, A., Cummings, M., Vancriekinge, M., Timms, W., and Maggio, J. E. (1995) *Biochemistry* **34**, 5191–5200
38. Deleted in proof
39. Zagorski, M. G., Shao, H., Ma, K., Yang, J., Li, H., Zeng, H., Zhang, Y., and Papolla, M. (2000) *Neurobiol. Aging* **21**, S10–S11 (Abstr. 48)
40. Zhang, S., Iwata, K., Lachenmann, M. J., Peng, J. W., Li, S., Stimson, E. R., Lu, Y., Felix, A. M., Maggio, J. E., and Lee, J. P. (2000) *J. Struct. Biol.* **130**, 130–141
41. Fancy, D. A., and Kodadek, T. (1999) *Proc. Natl. Acad. Sci. U. S. A.* **96**, 6020–6024
42. Fancy, D. A. (2000) *Curr. Opin. Chem. Biol.* **4**, 28–33
43. Fezoui, Y., Hartley, D. M., Harper, J. D., Khurana, R., Walsh, D. M., Condron, M. M., Selkoe, D. J., Lansbury, P. T., Fink, A. L., and Teplow, D. B. (2000) *Amyloid* **7**, 166–178
44. Colon, W., and Kelly, J. W. (1992) *Biochemistry* **31**, 8654–8660
45. Fancy, D. A., Denison, C., Kim, K., Xie, Y. Q., Holdeman, T., Amini, F., and Kodadek, T. (2000) *Chem. Biol.* **7**, 697–708
46. Zhang, X. Y., and Rodgers, M. A. J. (1995) *J. Phys. Chem. A* **99**, 12797–12803
47. Tanielian, C., Wolff, C., and Esch, M. (1996) *J. Phys. Chem. A* **100**, 6555–6560
48. Le Châtelier, H. L. (1884) *Comptes Rendus* **99**, 786
49. Le Châtelier, H. L. (1888) *Annales des Mines* **13**, 157
50. Kelly, J. W., Colon, W., Lai, Z., Lashuel, H. A., McCulloch, J., McCutchen, S. L., Miroy, G. J., and Peterson, S. A. (1997) *Adv. Protein Chem.* **50**, 161–181
51. Colon, W., Lai, Z., McCutchen, S. L., Miroy, G. J., Strang, C., and Kelly, J. W. (1996) *Ciba Found. Symp.* **199**, 228–238
52. Lai, Z., McCulloch, J., Lashuel, H. A., and Kelly, J. W. (1997) *Biochemistry* **36**, 10230–10239
53. Peterson, S. A., Klabunde, T., Lashuel, H. A., Purkey, H., Sacchettini, J. C., and Kelly, J. W. (1998) *Proc. Natl. Acad. Sci. U. S. A.* **95**, 12956–12960
54. McLaurin, J., Yang, D. S., Yip, C. M., and Fraser, P. E. (2000) *J. Struct. Biol.* **130**, 259–270
55. Rochet, J. C., and Lansbury, P. T., Jr. (2000) *Curr. Opin. Struct. Biol.* **10**, 60–68
56. Chiti, F., Taddei, N., Webster, P., Hamada, D., Fiaschi, T., Ramponi, G., and Dobson, C. M. (1999) *Nat. Struct. Biol.* **6**, 380–387

---

[3] G. Bitan and D. Teplow, submitted for publication.